

MICROSATELLITE AUTONOMOUS GNC IN-FLIGHT VALIDATION

**Franck DARNON⁽¹⁾, Jean-Charles DAMERY⁽¹⁾, Christine FALLET⁽¹⁾, Clémence
LE FEVRE⁽¹⁾, Réjane IBOS⁽¹⁾ and Denis LAURICHESSE⁽¹⁾**

⁽¹⁾Centre National d'Etudes Spatiales, 18 avenue E. Belin, 31401 TOULOUSE, France,
+33.5.61.28.30.78, franck.darnon@cnes.fr

Abstract: *The flight software of the currently in-flight PICARD microsatellite has been modified in order to test an autonomous Guidance, Navigation & Control (GNC). This new GNC includes the following functions: orbit extrapolation, reference frame conversion, Moon and Sun ephemerides computation, 6 standard pointing computations and the management of guidance discontinuities, including sensor dazzling avoidance. This GNC has been uploaded and successfully in-flight tested in March 2014, during a 15-day campaign, demonstrating the performances and robustness of the concept.*

Keywords: *Guidance, Navigation, Autonomy*

1. Introduction

In the frame of satellite decommissioning preparation, CNES¹ offers opportunities to perform experiments on operational satellites. The autonomous GNC² demonstration has been performed in this context. Decided in April 2013 the experiment was carried out on board the PICARD microsatellite (Fig. 1) in March 2014.

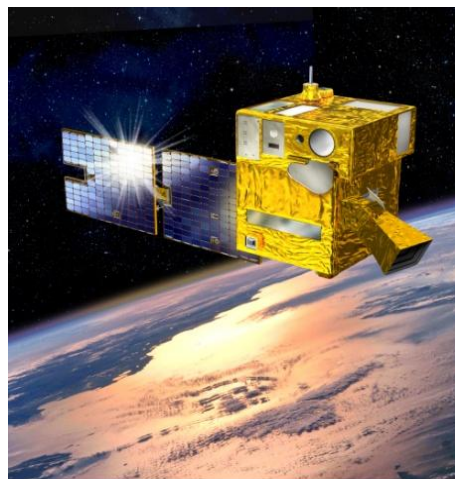


Figure 1. PICARD microsatellite

¹ CNES : Centre National d'Etudes Spatiales

² GNC : Guidance, Navigation & Control

Going toward a higher level of on-board autonomy is of major interest for satellites. For what concerns the Guidance, Navigation & Control (GNC) functions, more spacecraft autonomy allows:

- To reduce the constraints for up-link contact and consequently: less ground operations, less ground station booking (number of passes and telecommand volume to upload), an increased spacecraft reliability in case of temporary link loss...
- To enhance the pointing accuracy, using up-to-date orbital data for computing the targeted attitude.

The purpose of the autonomous GNC experiment is to upgrade the PICARD flight software in order to test and validate an autonomous GNC, allowing the satellite to follow various standard pointing modes with very few (even no more) ground GNC telecommands.

This paper will address the experiment context, the GNC function implementation including their ground validation, and by the end, the in-flight results.

2. Context

2.1. The PICARD microsatellite

Launched in June 2010, PICARD is a microsatellite designed for sun observation [1] operating on a quasicircular sun-synchronous low Earth orbit (700 km altitude). Based on the generic MYRIADE microsatellite bus (150 kg class), it belongs to the 20 MYRIADE-based microsatellite set which have flown or are in development [2] since 2004.

2.2. The PICARD Experiment constraints and challenges

Planning

Due to the short time lap between the decommissioning decision and the effective satellite end-of-life operations, the experiments had to be prepared and run within a tight planning. In the case of PICARD autonomous GNC experiment, the design, development, validation and experiment phases were carried out in less than one year.

Re-use of an existing system

The End-Of-Life experiments had to deal with the system as is, which implies, as far as possible, to not change the satellite operational modes, the ground-board interfaces, the ground segment... Moreover, they had to deal with hardware constraints. For the autonomous GNC experiment, the most severe one were:

- No embedded GNSS³ equipment which leads to no available in-flight measured orbital data;
- Optical sensors not robust to Earth, Sun or Moon dazzling. Consequently the autonomous GNC computation methods have to be robust to sensor dazzling;
- An on board computer with limited resources (memory size and CPU load in a real time environment).

³ GNSS: Global Navigation Satellite System

2.3. The PICARD autonomous GNC Experiment objectives

The experiment purpose aims to increase the level of the satellite autonomy, implementing the configuration represented figure 2, as an intermediate step towards a full autonomous system.

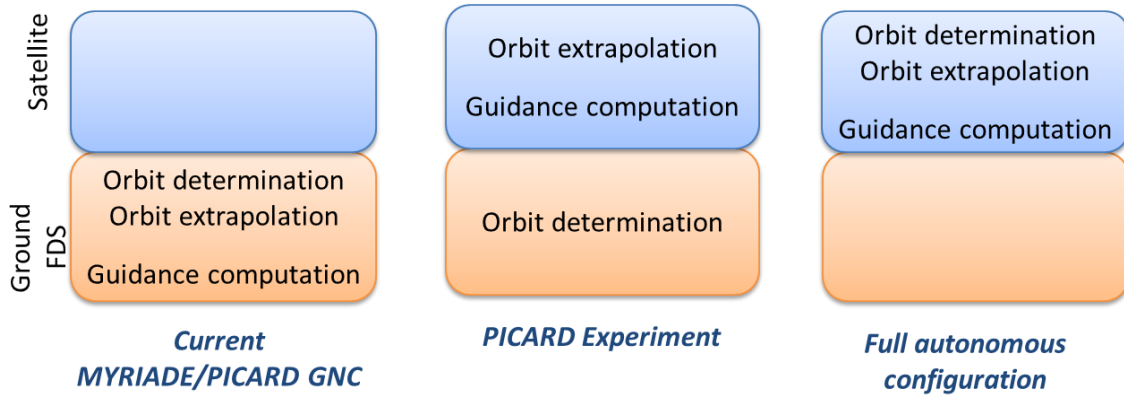


Figure 2. Different possible GNC configurations (ground/board sharing)

3. PICARD GNC experiment overview

3.1. Current MYRIADE/PICARD GNC

The current MYRIADE GNC is illustrated figure 3.

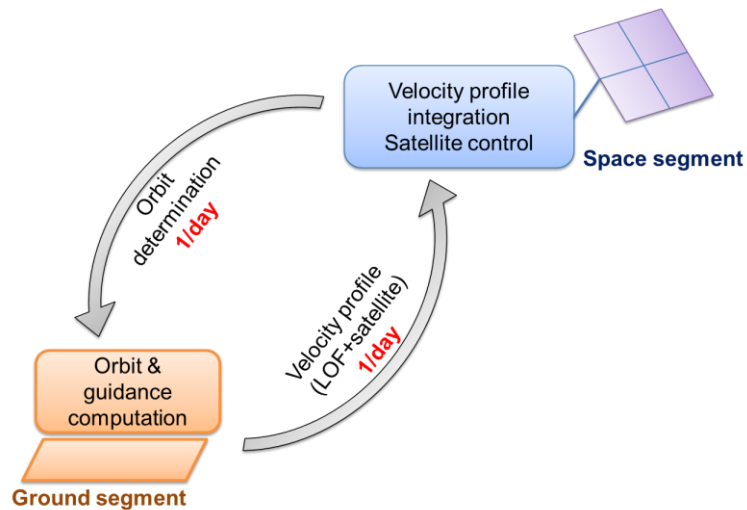


Figure 3. The Current MYRIADE/PICARD GNC

It includes:

- Ground orbit determination, based either on GNSS flight data (when a GNSS is embedded) or S-band telemetry ranging (PICARD case);
- Ground orbit extrapolation;
- Ground computation of the satellite guidance profile;
- Orbit (LOF⁴) and guidance uploading to the satellite (typically from 1 time/day up to 1/week);

The satellite attitude control is based on a 3-axis stabilization with a star tracker for attitude measurement and reaction wheels for control (in nominal mode). The control loop is synchronized on a 4 Hz clock [3].

The LOF and guidance are uploaded in the following format:

- A reference attitude quaternion;
- A velocity profile represented either in a polynomial or in a harmonic (based on the orbital pulsation) form.

The LOF, is expressed w.r.t. an inertial reference frame.

The guidance is expressed either w.r.t. an inertial reference frame or w.r.t LOF.

This way of commanding the satellite attitude implies errors on the on-board guidance, e.g. due to the harmonic guidance form which does not perfectly fit the desired profile.

3.2. PICARD Experiment objectives

The purpose of the PICARD GNC experiment is to overpass the current configuration limitations, having no more guidance uploading constraints and a more precise satellite pointing. This can be achieved if the orbit and the attitude guidance are on-board computed. As there is no embedded GNSS on PICARD satellite, an alternative architecture, with the orbit remaining ground estimated, has been tested:

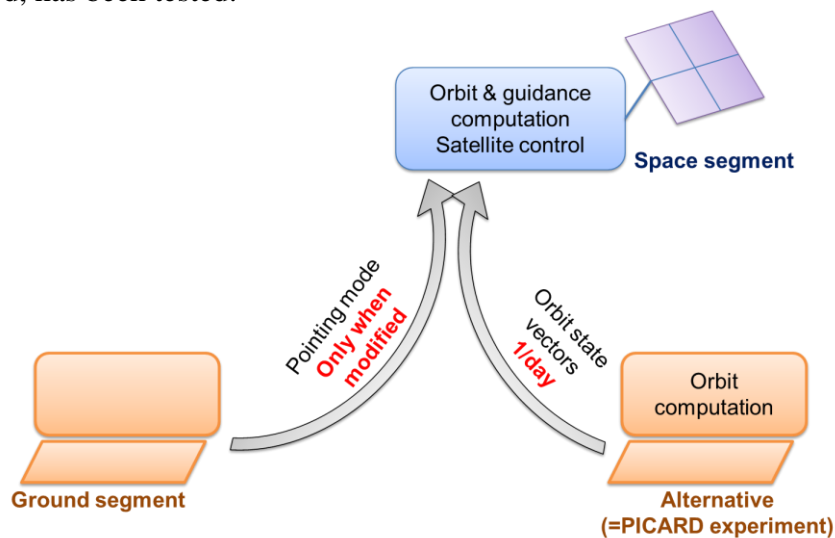


Figure 4. The Experimental PICARD GNC overview

⁴ LOF: Local Orbital Frame

The alternative architecture, tested on PICARD suits with both configurations :

- Spacecrafts with no embedded GNSS;
- Spacecrafts with GNSS but requiring maintaining the mission (possibly in a performance degraded mode) in case of GNSS equipment failure.

3.3 Development and Validation plans

The following phases have been carried out:

Definition of the experiment

This two month initial phase includes the definition of:

- the general GNC architecture;
- the functions to implement and their associated computing methods;
- the ground-board interfaces (TM/TC⁵) to adapt or to add ;
- the satellite data base evolutions;
- the experimental GNC FDIR⁶;
- the experimental plan.

Development of the new GNC functions

The 6-month development phase has been performed using the MATLAB®/Simulink environment, on the basis of a simplified PICARD AOCS⁷ simulator.

Integration to the flight software

The GNC flight software has been automatically generated from the MATLAB®/Simulink model.

This code has been integrated into the existing flight software and other services have been implemented (TM/TC, FDIR...). As a consequence of the autonomous GNC calculations, the CPU⁸ load has risen from about 50% up to more than 80% with an operating autonomous GNC. The computation time for the autonomous GNC tasks (orbit and guidance functions) is exceeding 100 ms (for a 4 Hz real time process), highlighting the consequent weight these new functions are representing. As a consequence, some optimizations had to be performed: rearrangement of the different sub-time slots, such as to guarantee a proper execution (in due time) of the different AOCS tasks.

Moreover, the autonomous GNC implementation into the flight software has resulted in increasing its binary size by 25%, which also required some optimization, not to exceed the maximum allowable size.

It can be noticed that these limitations are coming from the quite low performances of the MYRIADE On Board Computer (developed in the late 90's) in comparison with the current state of the art. Equivalent constraints are not expected on more recent hardware.

⁵ TM/TC: Telemetry/Telecommand

⁶ FDIR : Fault Detection Isolation and Recovery

⁷ AOCS : Attitude and Orbite Control system

⁸ CPU : Central Processing Unit

Validation

The validation has been performed in four steps:

At elementary function level (orbit and guidance)

The MATLAB®/Simulink models have been compared to reference data generated thanks to CNES reference libraries: BOLERO [4] and CELESTLAB [5] for orbit and PATRIUS [7] for guidance.

The objectives assigned were to validate the new models (both unitarily and coupled) developed in the frame of the PICARD experiment. An additional objective was also to check the general behavior of the GNC when coupled to the simplified MATLAB®/Simulink AOCS simulator, such as, for instance, to tune the GNC parameters.

At AOCS level

The GNC code, automatically generated from the MATLAB®/Simulink models, has been integrated into the PICARD AOCS FORTRAN simulator, which is out of MATLAB®/Simulink environment.

The objective was to validate the global GNC/AOCS behavior, especially when running the full experimental plan.

At software level

The new software has been run on the software validation bench.

The objective was to measure the software performances and to validate the new functions, through a comparison with reference results produced on the AOCS simulator.

At satellite level

The new flight software has been loaded and tested on the satellite simulation bench.

The objectives were to validate the general satellite behavior, including, the TM/TC management, the FDIR, the absence of regression on other functions...

4. Autonomous GNC detailed definition

4.1. Autonomous GNC Overview and Interfaces

The general architecture is provided figure 5. Using initial orbit state vectors and a pointing mode as inputs (telecommanded), it computes firstly the current satellite position, then the satellite guidance attitude to feed the attitude control function.

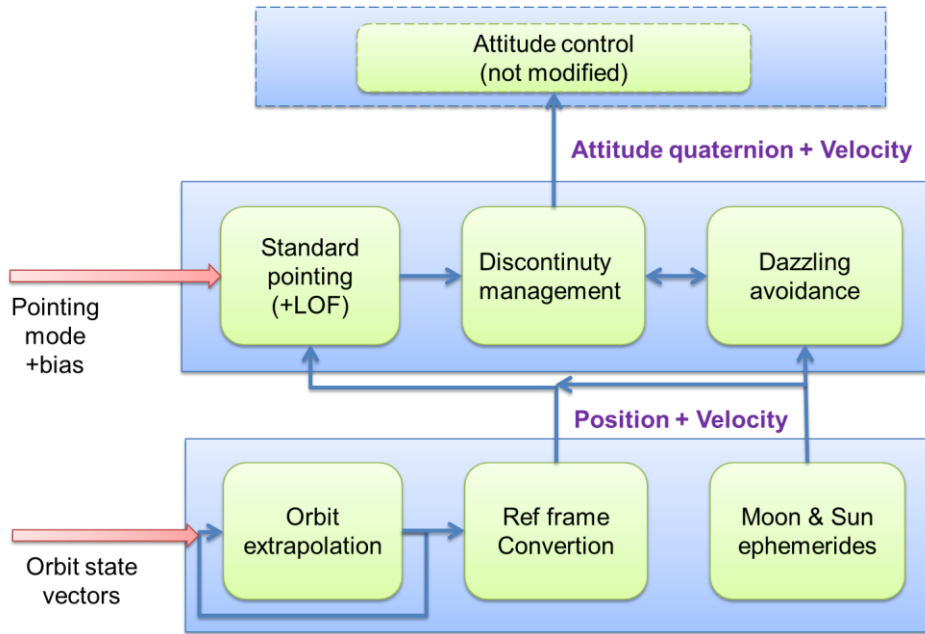


Figure 5. GNC functional diagram and main interfaces

4.2. Orbit extrapolation function

The orbit extrapolation function is propagating, at the AOCS clock (i.e. @4Hz), the ground periodically updated satellite orbit ephemeris (position, velocity) in the ITRF⁹ terrestrial frame. It has been chosen to work with orbit data inputs represented in a terrestrial frame (ITRF), in order to be as close as possible to an architecture dealing with a GNSS provided orbit (see figure 2: full autonomous configuration). Indeed, considering the required accuracy, the GNSS WGS84 frame and the ITRF frame can be considered as equivalent. Consequently, the autonomous GNC kit developed in the frame of this experiment can directly be re-used and interfaced with satellites using GNSS data to deliver the orbit.

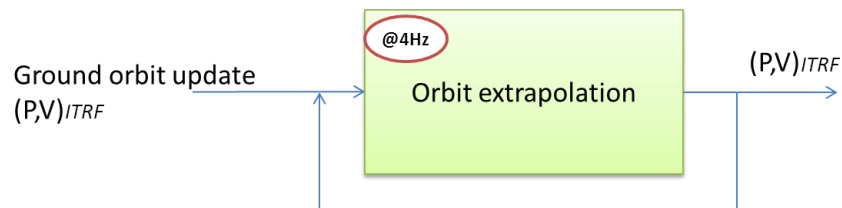


Figure 6. Orbit extrapolation function

Extrapolation model trade-off

A 6 order gravitational model and a Runge-Kutta integration (order 6) have been selected. The already flight proven CNES “BOLERO” library [4] has been reused. By comparing the extrapolation results with a fine orbit propagation using the CNES reference tool (ZOOM

⁹ ITRF : International Terrestrial Reference Frame

software), it has been shown that the 6x6 order model is the best compromise between performances and computation load. Moreover a more precise model representing drag effect would imply to upload the drag coefficients to the satellite, which is in contradiction with the autonomy objectives.

Orbit update frequency determination

The orbit is determined by the ground, typically 1 time per day, then 6x6 model is adjusted on a short time span (few hours) for computing N orbital state vectors (position, velocity) in the terrestrial ITRF frame with a given time gap. These orbit parameters are then uploaded to the satellite as illustrated on figure 7. By using the same model to adjust the ground ephemerides and the on-board extrapolation, the consistency between the two orbits is ensured.

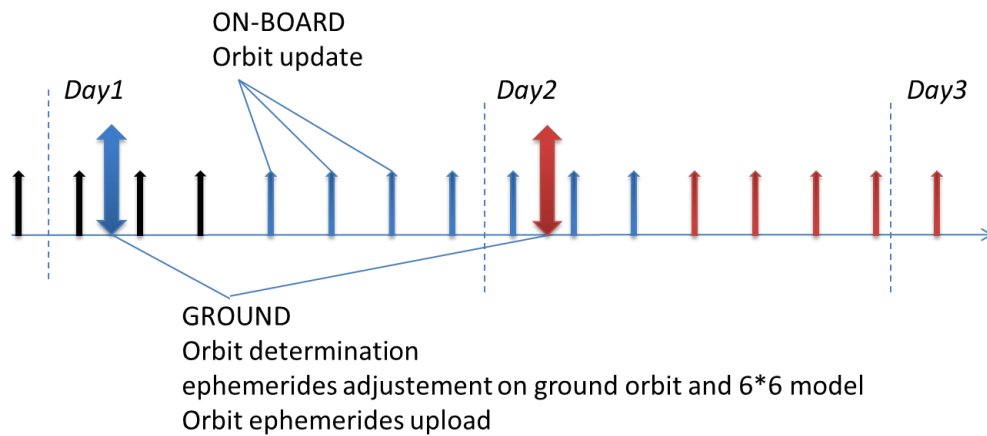


Figure 7. Orbit update chronology

A trade-off has concluded in choosing a 4-hour time gap between two orbit updates. During the PICARD experiment, a 2-hour time gap has also been tested in order to measure further orbit accuracy gain that can be expected when uploading up to 12 orbital state vectors per day.

Time gap between to orbit update	RMS long-track error
2h	~20m
4h	~50m
8h	~100m

Table 1. Expected orbit error as a function of orbit update frequency

4.3. Reference frame conversion function

The reference frame conversion function is transforming, at the AOCS clock frequency (i.e. @4Hz), the orbit position and velocity into an inertial frame (GCRF¹⁰).



Figure 8. Reference frame conversion function

Three successive frame conversions are performed:

- ITRF to TIRF : For a high accuracy, it can take into account the CIP¹¹ coordinates (X_p, Y_p) (IERS bulletins and tide impacts);
- TIRF to CIRF : For a high accuracy, it can take into account the UT1¹²-UTC¹³ gap (IERS¹⁴ bulletins and tide impacts);
- CIRF to GCRF : taking into account the precession and nutation effects on the Earth equatorial plan, using IERS bulletin (X, Y) giving the Earth rotation axis orientation. For a high accuracy, some corrective terms can be applied (dX, dY).

On the basis of a performance analysis, carried out using the CNES CELESTLAB reference tool [5], a trade-off has concluded to take into account the UT1-UTC gap, but not the tide effects nor the CIP coordinates (X_p, Y_p) and the corrective terms (dX, dY). Typically 15 m accuracy is expected (on the Earth equator).

Model simplification : take into account			Angular error [mas] vs. precise model	Distance error (@equator) [m] vs. precise model
(X _p , Y _p)	UT1-UTC gap	(dX, dY)		
Yes	Yes	No	0.284	8.8E-03
No	Yes	No	484.3	15.0
No	No*	No	13546.0	418.9

*Considering UT1-UTC max (0.9s)

Table 2. Simplified frame conversion accuracy

¹⁰ GCRF : Geocentric Celestial Reference Frame

¹¹ CIP : Celestial Intermediate Pole

¹² UT1 : Universal Time

¹³ UTC : Coordinated Universal Time

¹⁴ IERS : International Earth Rotation and Reference Systems Service

4.4. Moon and Sun ephemeris computation

The Moon and Sun positions are computed in the GCRF reference frame, each 10 s using MEEUS analytical models [6].

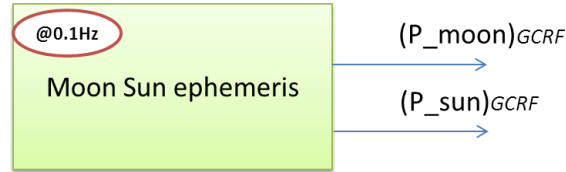


Figure 9. Moon and Sun ephemerides computation function

For the Moon direction computation, a “medium” accuracy has been selected, as there is no requirement for a high accuracy (the Moon direction is used for the GNC sensor dazzling avoidance function).

Compared to an accurate JPL¹⁵ numerical model (DE423), the expected MEEUS model performances are the following:

Model	Longitude [arcsec]	Latitude [arcsec]	Distance [km]	Angle GCRF [arcsec]
Moon (medium)	108	112	225	121
Sun	37.4	1.2	12000	37.9

Table 3. Moon and Sun ephemerides accuracy

4.5. Standard pointing computation



Figure 10. Standard Pointing computation function

¹⁵ JPL : Jet Propulsion Laboratory

Local Orbit Frame (LOF)

The function is computing, at the AOCS clock (i.e. @4Hz), the Local Orbital Frame (LOF) attitude, defined as

- Z_{LOF} directed toward the Earth center;
- Y_{LOF} anti-normal to the Earth plane.

Standard Pointings

Among 6 standard pointing (depending of the Pointing Mode selected by ground TeleCommand), a standard attitude is computed at the AOCS clock (i.e. @4Hz):

- **GEOCENTRIC** pointing = LOF attitude
- **HELIOCENTRIC** pointing:
 - Z_{SAT} directed toward the Sun (direction provided by the Sun ephemeris function)
 - X_{SAT} in the orbit plane toward the south
- **TRACK COMPENSATION** pointing: based on the LOF, including a yaw rotation (around Z_{SAT}) such as to compensate the Earth rotation, i.e. having the Y_{SAT} axis projection on the Earth surface perpendicular to the ground track. The yaw rotation angle is computed assuming a spherical Earth with a constant angular velocity.
- **NADIR** (or geodetic) pointing :
 - Z_{SAT} normal the Earth surface, assuming an ellipsoidal Earth.The Z_{SAT} direction is computed with an iterative method.

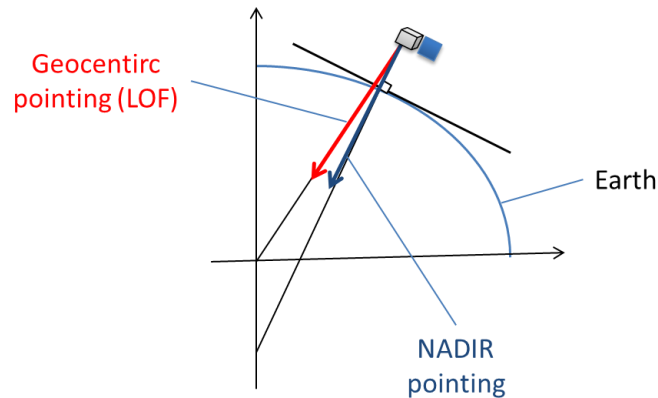


Figure 11. Nadir (geodetic) pointing definition

- **YAW STEERING** pointing: based on the LOF, including a yaw rotation (around Z_{SAT}) such as to have Y_{SAT} perpendicular to the sun direction (provided by the Sun ephemeris function). This Yaw Steering pointing is used when there is no mission constraint concerning the yaw angle but computed such as to optimize the solar array illumination.
- **INERTIAL** pointing: constant attitude w.r.t. GCRF inertial frame

Whatever the standard pointing selected, the attitude quaternion: $Q_{Standard\ Pointing}(t)$ is represented w.r.t. GCRF inertial frame.

Pointing Bias

Then, an attitude bias may be applied on the standard pointing in order to compute the targeted attitude.

$$Q_{Targetted\ Attitude\ t} = Q_{Standard\ Pointing\ t} * Q_{bias} \quad (1)$$

This bias is ground TeleCommanded, either in case of different axis convention, or when an angular tilt has to be applied for mission purpose. Another case of bias utilization is for orbital manoeuvres: For instance, a geocentric pointing with bias can be commanded such as to align the thrust in the required direction.

4.6. Guidance discontinuity management (including sensor dazzling avoidance)

The attitude discontinuity management function is ensuring a “continuous” guidance attitude quaternion, in case of:

- Change of the standard pointing mode (e.g. from heliocentric to geocentric pointing);
- Change of the bias (e.g. from geocentric to geocentric + bias for an orbital maneuver).

The attitude discontinuity management function take into account:

- The kinematic allocations;
- The sensor dazzling avoidance.

This function is computing, at the AOCS clock frequency (i.e. @4Hz), the attitude guidance quaternion (represented w.r.t. GCRF inertial frame) as well as the guidance frame velocity, w.r.t. GCRF frame and expressed into the satellite frame.

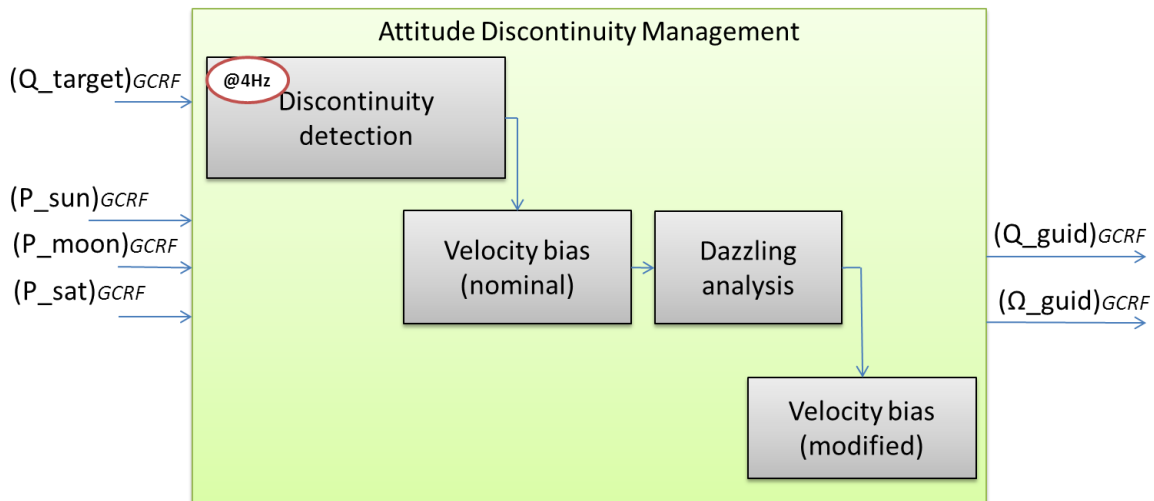


Figure 12. Discontinuity management (inc. sensor dazzling avoidance)

Discontinuity Detection

An angular comparison between the current targeted attitude and previous time step guidance attitude is made. Not exceeding an angular threshold (typically 1°), the guidance attitude equals the targeted attitude. Otherwise, the following steps apply.

Velocity Bias (nominal)

When a discontinuity is detected, the guidance attitude equals the previous time step guidance attitude on which a rotation is applied. This rotation has the following characteristics:

- Orientation: Such as to reach the targeted attitude by the shortest angular way. The direction is adjusted at each time step in case of a non-constant targeted attitude;
- Magnitude: Such as to be feasible taking into account the satellite kinematics capabilities.

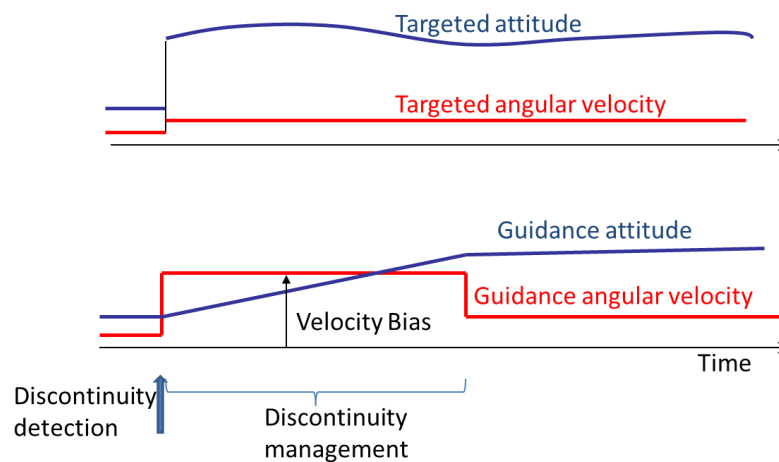


Figure 13. Attitude guidance discontinuity management principle

The major drawbacks of this method are:

- 1- A non-time optimal slew, on the contrary of an iterative method globally optimizing the slew path and rate (e.g. taking into account a non-constant targeted attitude as well as dynamic kinematics capabilities).
- 2- Angular velocity discontinuities at the slew bounds.

As the purpose of this function is to smoothly on-board manage the attitude transient between two standard pointings, without severe time or attitude constraints, it has been decided to not implement an optimized (even optimal) method which would have imply a global slew asynchronous computation. Generally speaking, such optimized methods are not intended to be implemented on board. Indeed, even in case of agile missions, requiring to make the best use of satellite kinematics capabilities, the mission planning being strongly coupled with the mission user needs, we expect the mission planning (inc. attitude) to remain (at least partly) ground commanded.

The velocity bias has been tuned such as:

- to guarantee the satellite controllability;
- to guarantee the guidance algorithm convergence, for all standard pointing transitions;
- to limit the attitude control error at the slew bounds due to velocity discontinuities.

Dazzling Analysis and Velocity Bias modification

In general, the guidance discontinuity management function has to take into account any satellite attitude constraints, such as:

- preventing optical sensor dazzling;
- preventing payload dazzling;
- limiting the viewing factor of radiative surfaces with Earth or Sun;
- etc...

Obviously, the GNC design and methods for managing the attitude discontinuities have to be adapted to the constraints to deal with, but some general concepts can be reused, such as those developed for the autonomous GNC PICARD experiment.

In the peculiar case of PICARD, the AOCS is using a star tracker with two optical heads (oriented in opposite directions) which are not delivering a valid estimated attitude when a bright object (Earth, Sun or Moon) crosses their field of view.

The method implemented in the PICARD experimental GNC consists, at each AOCS time step (@4 Hz), in:

- Computing the guidance attitude with the nominal velocity bias applied;
- Evaluating the 2 sensor heads angles w.r.t. 3 bright objects and comparing with angular thresholds;
- If the 2 heads are simultaneously dazzled, determining which bright object is responsible for the dazzling status change (w.r.t. previous time step);
- Determining the rotation sign to apply. This sign depends on the relative geometrical configuration between the nominal velocity bias, the sensor axis and the bright object direction;
- Computing the guidance attitude, based on the previous time step attitude and applying a rotation around +/- the bright object direction.

This sensor dazzling avoidance principle is represented figure 14, in a simplified manner (the nominal velocity bias vector as well as the satellite-bright object direction are not constant). It can be described as making the sensor “rotate” around the bright object excluding cone, through the shortest way, to reach the targeted attitude.

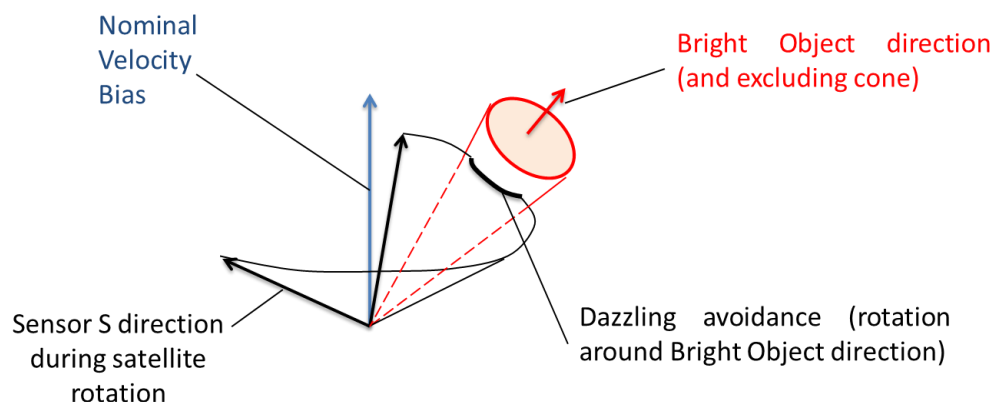


Figure 14. Sensor dazzling avoidance principle

4.8. Attitude control

The attitude control function has not been modified in the frame of this experiment, as the interfaces have remained unchanged (attitude quaternion and velocity represented in an inertial frame).

5. In-flight results

5.1. Experiment plan

The in-flight experiment was carried out from March 10 to March 25, 2014. It consisted in:

- Testing all the standard pointing during several orbits each;
- Changing the attitude bias (about 30 times) such as to test the attitude discontinuity management for various direction, amplitude and bright objects avoidance (5 occurrences);
- Commanding alternatively two different pointing modes on each orbit during a several day period;
- Reproducing some PICARD payload calibration sequences requiring specific attitude profiles, but using the autonomous GNC.

5.2. Experiment results

The new flight software including the autonomous GNC works perfectly in orbit.

The transitions between the ground-guided and the autonomous GNC modes took place without any problem. The flight software has operated without exceeding the computation resources, even the computation load of the new GNC tasks was drastically increased compared to the previous one.

The expected level of accuracy for the on-board orbit has been reached. Figure 15 presents the difference between the orbital position (in GCRF frame) obtained from the satellite telemetry and the orbital position predicted by the ground segment with the precise orbit dynamical model. The discontinuities are explained by the orbit updates (every 2 hours in this case).

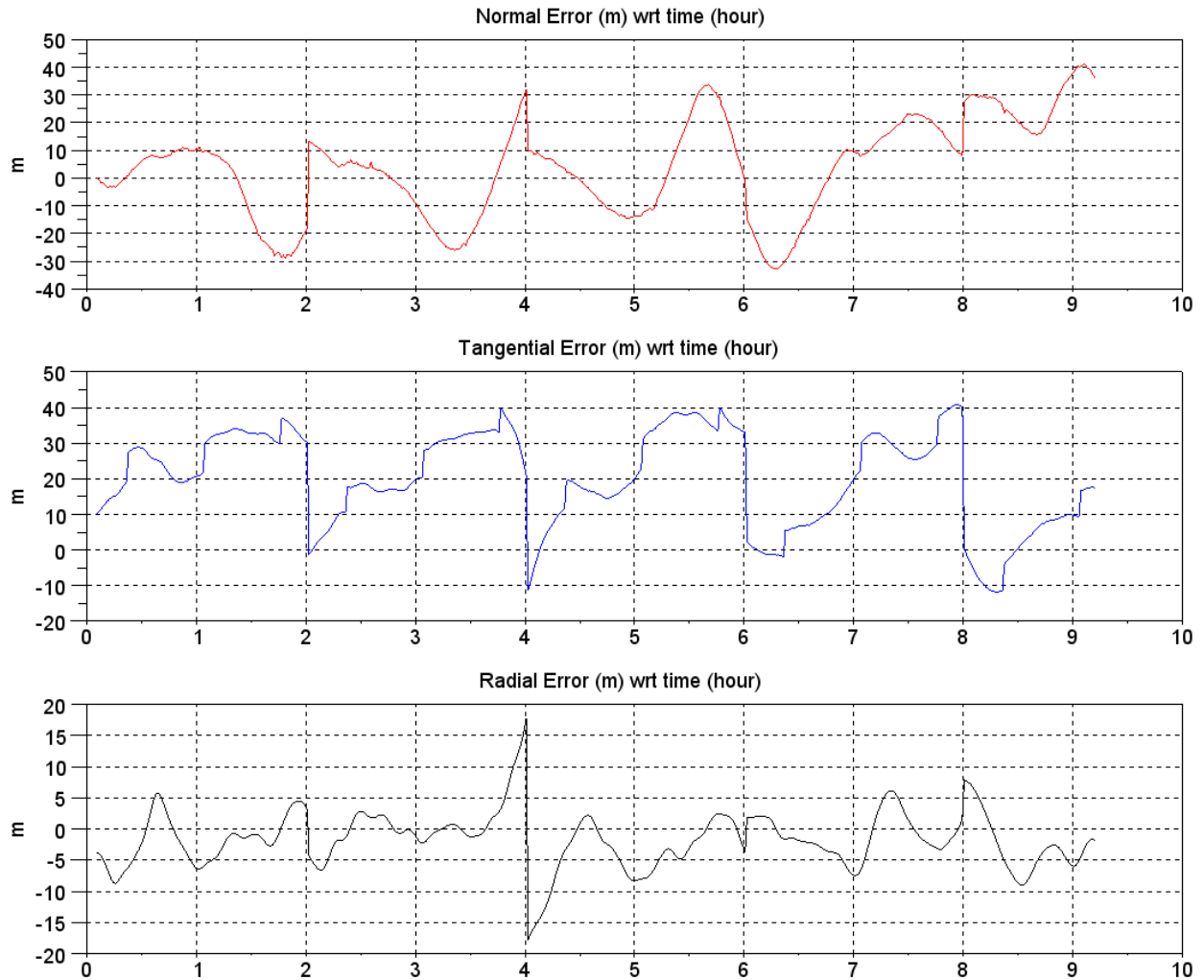


Figure 15. Measured orbit error as a function of time

The attitude control system perfectly worked whatever the guidance commanded, including the velocity bias during pointing mode changes. Moreover, the two sensor heads were never simultaneously dazzled.

As an example, the satellite telemetry corresponding to a sequence starting from a heliocentric pointing is represented figures 16 to 19. Two orders are sent: First to command an off pointing (about 180°), then to go back to the previous heliocentric attitude, as it can be seen on the targeted attitude computed by the satellite GNC (figure 16).

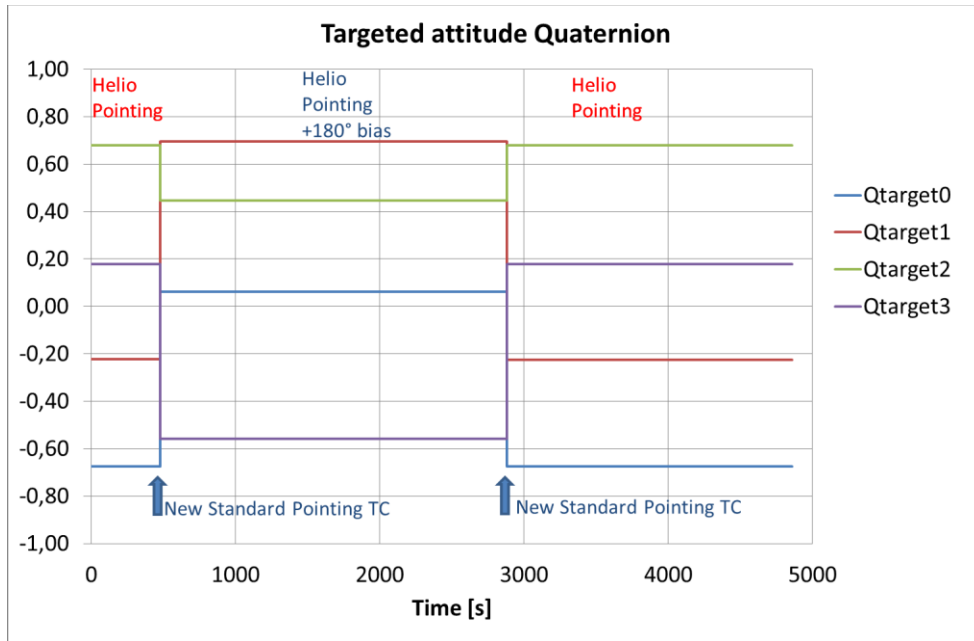


Figure 16. Targeted attitude as a function of time

The GNC discontinuity management function properly managed the attitude transitions, as it can be seen figure 17 on the guidance attitude quaternion compounds which are continuous:

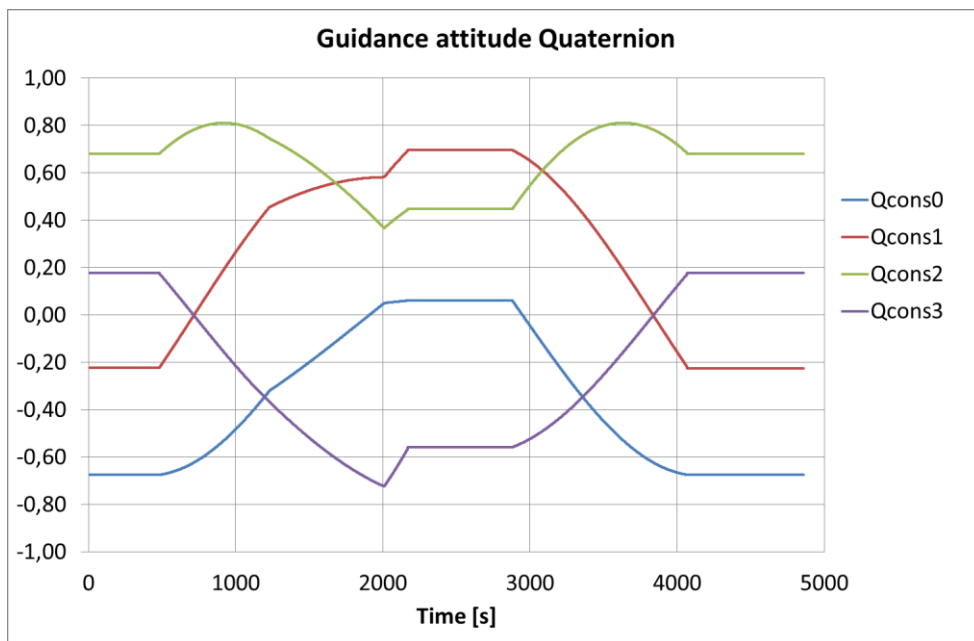


Figure 17. Guidance attitude quaternion as a function of time

Different GNC modes successively took place, as highlighted when looking to the guidance velocity figure 18:

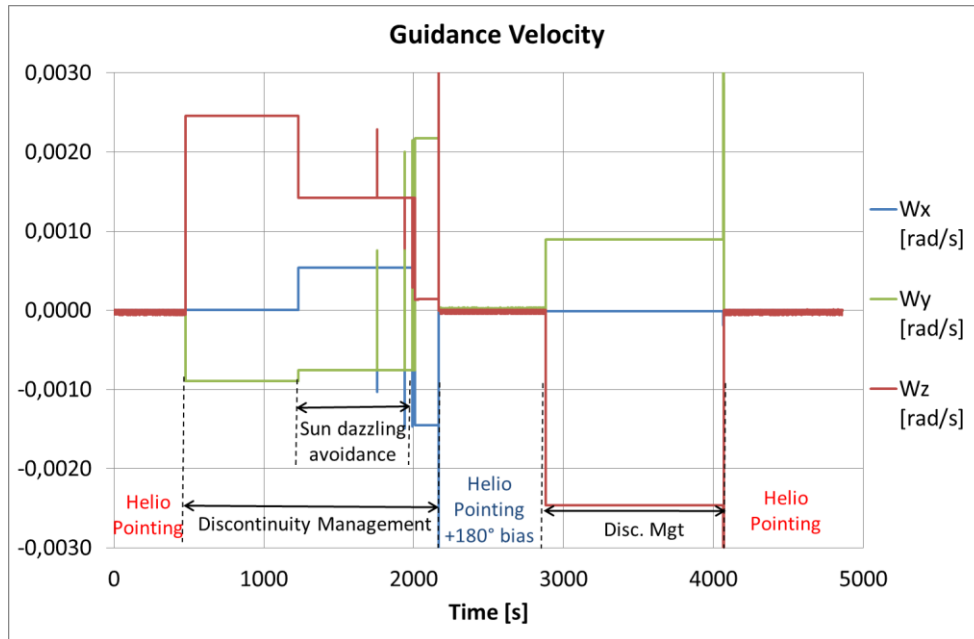


Figure 18. Guidance Velocity as a function of time

The first 180° slew had to deal with a sun dazzling on the second sensor optical head (the first being dazzled by the Earth). Consequently, the GNC temporarily commanded a change in the rotation axis and velocity. On the contrary, the second attitude transition was managed without dazzling issue, leading to an almost constant rotation axis.

As the GNC is not guaranteeing angular velocity continuity, the GNC mode transitions implied some attitude control errors. Figure 19 is representing the angular difference between the guidance quaternion and the satellite attitude, estimated on the basis of star tracker measurements. Each time a bias velocity is applied, a reproducible error (about 0.9°) occurred and was rapidly damped. The amplitude directly results in the velocity bias tuning.

When a change in the rotation direction or velocity occurs, e.g. in case of dazzling avoidance, another control error can take place. In this peculiar case, the second error peak reached 1.1° , as the consequence of the significant velocity step at the end of the dazzling avoidance mode, as it can be seen on figure 18 (sign change of the X and Y satellite velocity compounds).

On figure 19, one can notice other error control peaks. They are not the result of the autonomous GNC computation methods, but the satellite attitude estimate, which is less accurate in case of star tracker optical head switch (change of the optical head not dazzled by Earth).

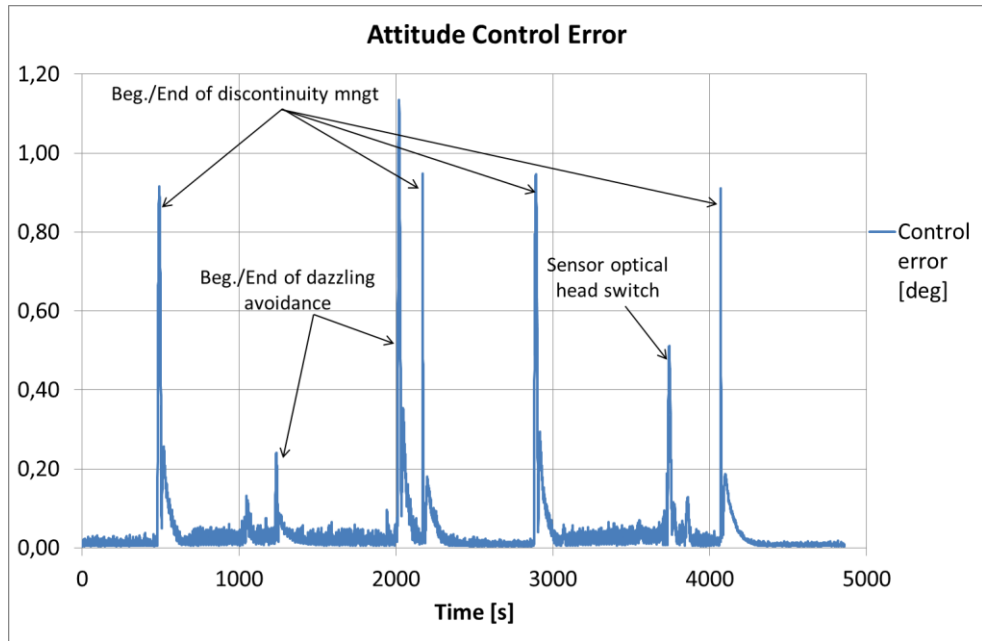


Figure 19. Attitude control error as a function of time

5.3. Orbit / Guidance functions performances

Three configurations (schematically represented figure 2) have been compared

- 1- The MYRIADE/PICARD current one with the Orbit and Guidance computed on ground and uploaded in a harmonic form;
- 2- The PICARD GNC experiment;
- 3- A full autonomous configuration with on-board orbit determination using GNSS data.

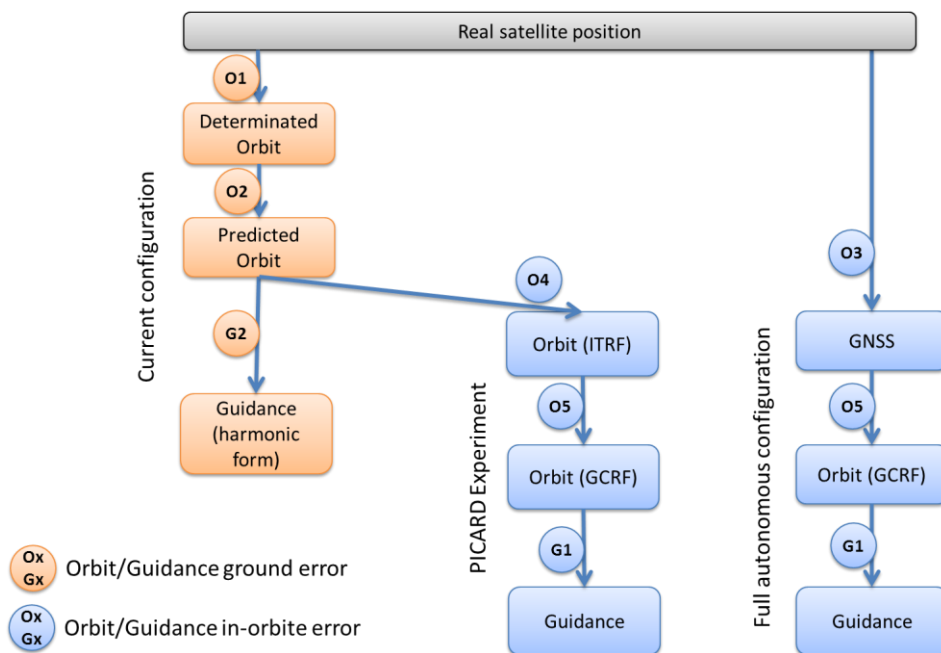


Figure 20. Contribution scheme to guidance error budget

Orbit Errors	Cross-track Error	Long-track Erreur	Altitude Error	Source
O1: On ground orbit determination	81 m	122 m	15 m	Typical value estimated for PICARD satellite, based on a descending DOPPLER ranging, using 6 different ground stations and 10 passes/day.
O2: On ground orbit prediction	195 m	405 m	45 m	Comparison between predicted et determined orbit: Average value for 12 day experiment Note the extrapolation error is much more correlated to the sun activity forecast error, than to the propagation horizon (1 to 3 days)
O3: On-board GNSS	10 m	10 m	10 m	Typical characteristics (after filtering)
O4+O5: On-board extrapolation + frame conversion	65 m	145 m	55 m	Comparison between the PICARD telemetry and the predicted orbit (on ground computed) The orbit is updated every 4 h.
O4+O5	38 m	47 m	27 m	The orbit is updated every 2 h.

Table 4. Orbit error evaluations

The main contribution to orbit errors comes from the on ground orbit extrapolation (O2 error) and uncertainties about the drag coming from the residual atmosphere (linked to the sun activity, which is not accurately predictable). The only way to improve the accuracy is to use on-board orbit measurement (GNSS).

The extrapolation and frame conversion functions implemented in the PICARD autonomous GNC experiment allows a rather good orbit computation (O4+O5 errors), which can be even improved by shortening the time period between two orbit updates. Then, the residual error is mainly a cross track one and is due to frame conversion (O4 error).

Guidance Errors	Geocentric	Track compensation	Yaw steering	NADIR	Heliocentric	Inertial	Source
G2: On ground guidance	200 μ rad	200 μ rad + 110 μ rad (yaw)	200 μ rad + 70 μ rad (yaw)	370 μ rad	350 μ rad (sun direction)	Numerical error	Different on going CNES missions with guidance velocity uploaded in a harmonic form
G1: On-board guidance (autonomous GNC)	<1 μ rad	<1 μ rad + 35 μ rad (yaw)	<1 μ rad + 70 μ rad (yaw)	8 μ rad	170 μ rad (sun direction)	Numerical error	Comparison between the guidance attitude (PICARD telemetry) with a reference attitude computed using the same orbit as an input

Table 5. Guidance error evaluations

As the ground-computed standard guidances are uploading using velocity harmonic profiles, their accuracy is rather low (G2 error). The on-board computation implemented in PICARD GNC experiment is significantly improving the guidance attitude accuracy, whatever the standard pointing.

A meaningful way to represent the guidance error of geocentric or nadir pointing missions is to evaluate the induced error at Earth surface (intersection between the line of sight and Earth surface), for instance for a 700 km altitude orbit.

2 geolocation errors can be defined, as represented figure 21:

- Predicted geolocation error: we are expecting to point towards A whereas we are pointing toward C. For instance, this error makes sense when the payload programming is associated to Earth flyby;
- Local geolocation error: the local geocentric (or nadir) attitude (corresponding to the real satellite position) should point toward B whereas we are pointing toward C. For instance, this error makes sense when it is important to be as close as possible to the local nadir, such as for altimetry mission (but no requirement to synchronize the payload programming to what was predicted to be pointed on Earth: A).

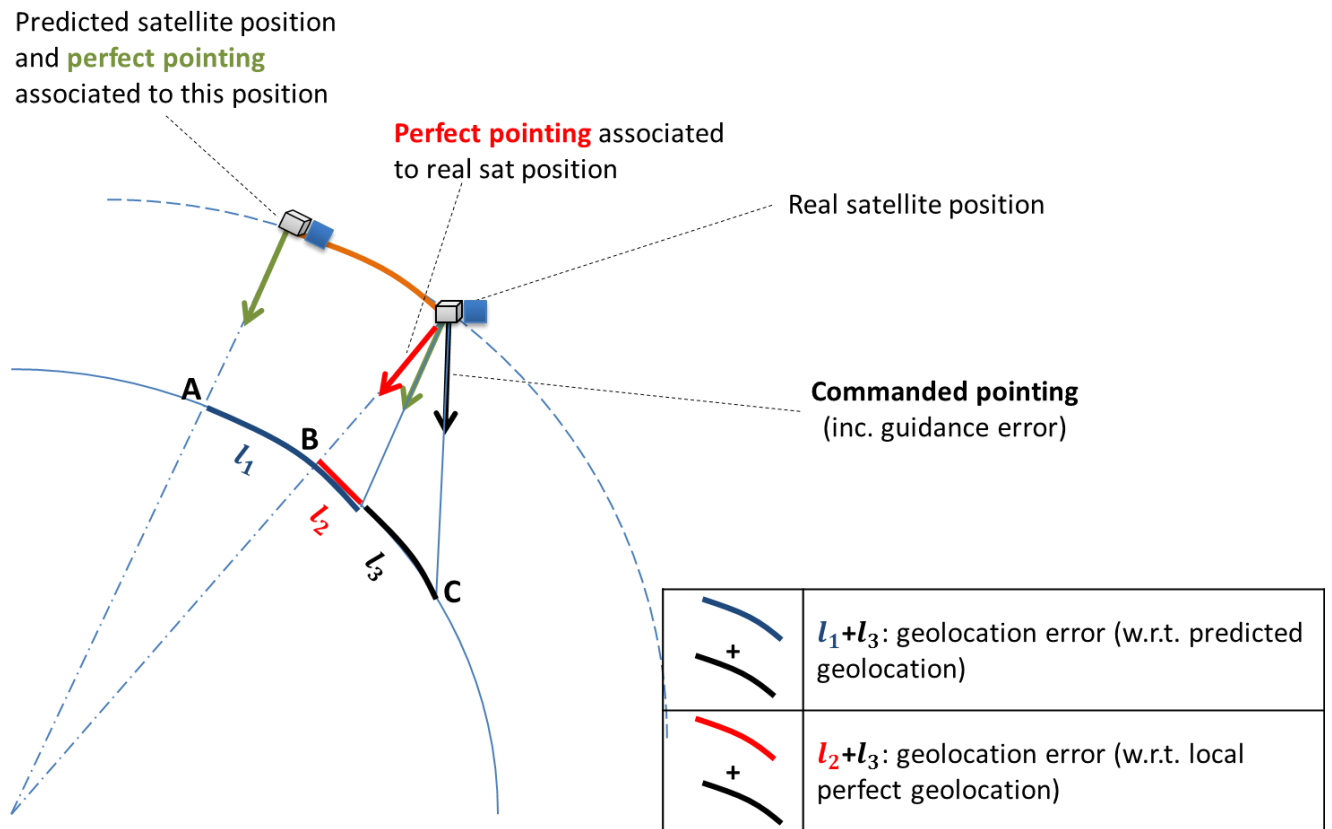


Figure 21. Geolocation error definition

	Current configuration O1+O2+G2				PICARD Experiment O1+O2+O4+O5+G1				Full autonomous configuration O3+O5+G1			
	Attitude error [μ rad]		Geoloc error @700km [m]		Attitude error [μ rad]		Geoloc error @700km [m]		Attitude error [μ rad]		Geoloc error @700km [m]	
GEOCENTRIC Pointing												
	predic ted	local	predic ted	local	predic ted	local	predic ted	local	predic ted	local	predic ted	local
Orbit	850	85	595	60	935	90	655	65	105	10	75	7
Guidance	200	200	140	140	0,1	0,1	0,1	0,1	0,1	0,1	0,1	0,1
Total	1050	285	735	200	935	90	655	65	105	10	75	7
NADIR Pointing												
	predic ted	local	predic ted	local	predic ted	local	predic ted	local	predic ted	local	predic ted	local
Orbit	850	85	595	60	935	90	655	65	105	10	75	7
Guidance	375	375	260	260	10	10	5	5	10	10	5	5
Total	1225	460	855	320	945	100	660	70	115	20	80	12

Table 6. Orbit and Guidance error evaluations for geocentric and nadir pointings

If we compare the current configuration to the autonomous GNC PICARD experiment:

- Marginal gain on the predicted geolocation error (**735 m** => **655 m**) for geocentric pointing. The on-board models contribution in the final orbit error budget remains limited (60m over 655m) since the main contributors are high uncertainties of Doppler measurements and solar activity forecast (595m). In the case of Picard experiment, the error induced by implementing a simplified orbit model on board (+60m) is largely balanced by the improvement obtained with the on-board guidance calculation (-140m).
- Gain on the predicted geolocation error (**855 m** => **660 m**) for nadir pointing linked to the poor nadir accuracy when uploaded using TC as harmonic form w.r.t. LOF.
- Significant gain on the attitude error w.r.t. the real local geocentric and nadir (respectively **285 μ rad** => **90 μ rad** and **460 μ rad** => **100 μ rad**). This error is less “orbit dependent”, consequently, we take full benefit of an improved guidance accuracy when it is on-board computed, especially for the nadir case.

“Extrapolating” the PICARD experiment to a full autonomous configuration, we expect further guidance accuracy improvements thanks to a better satellite position in-orbit estimation. For instance, in case of geocentric pointing, the predicted geolocation error is drastically reduced (**655 m** => **75 m**) as well as the local real geocentric direction error (**90 μ rad** => **10 μ rad**).

6. Conclusion

A new GNC, including orbit extrapolation, reference frame conversion, Moon and Sun ephemerides computation, 6 standard pointing computations and the management of guidance discontinuities, including sensor dazzling avoidance has been developed and in-flight tested in March 2014 on board the PICARD micro-satellite.

The most challenging aspects of this experiment was to develop a full autonomous and multi-mission GNC “kit” compliant with existing in-orbit satellites, with limited on-board resources and in less than one year (from the experiment decision up to in-flight operations).

This in-flight experiment has been successfully carried out and has demonstrated the capabilities and performances of such an autonomous GNC for low Earth orbit, and even at the scale of a microsatellite.

Compared to the current MYRIADE ground commanded guidance profiles, such an autonomous GNC offers many benefits:

- It significantly reduces the number of ground operations to handle, as well as the number of ground/board contacts for guidance profile uploading;
- It satisfies to various type of missions (different standard pointing), as a generic GNC (and consequently a generic ground segment);
- It complies with mixed ground/on board guidance commands, for instance part of the orbit using ground telecommanded guidance profiles (for mission purpose), and rest of the orbit using autonomous standard pointing;
- It is managing attitude guidance discontinuities, including sensor (or payload) dazzling avoidance, making the satellite robust to this kind of AOCS constraints;
- Whatever the pointing, the guidance accuracy is improved;
- It can be directly interfaced with GNSS data such as to further enhance the guidance performance and satellite autonomy.

7. References

[1] <http://smc.cnes.fr/PICARD/index.htm>

[2] Clair, M. A. and Bach, M., “The CNES microsatellite Product Line: MYRIADE”, 4S Symposium, 2006.

[3] Fallet, Ch. et al. “Myriade Microsatellite end-of-life as a flight test bench” 4S symposium, 2014.

[4] Pontet B. And Laurichesse D. “BOLERO: on board software library for space flight dynamic applications”. Proceedings of the Data Systems in Aerospace (DASIA) conference, Dublin, May 2002.

[5] CNES Space mechanics toolbox for mission analysis, CELESTLAB, issue 3, revision: 0.

[6] Astronomical algorithms, Jean Meeus, 1991.

[7] Denis, C. and Tanguy, Y. “The SIRIUS Flight Dynamics Library for the next 25 years”. Proceedings of the 5th International Conference on Astrodynamics Tools and Techniques (ICATT)